

Local mapping of strain at grain boundaries in colossal magnetoresistive films using x-ray microdiffraction

Yeong-Ah Soh^{a)}

NEC Research Institute, 4 Independence Way, Princeton, New Jersey 08540

P. G. Evans

Bell Laboratories, Lucent Technologies, Murray Hill, New Jersey 07974

Z. Cai and B. Lai

Argonne National Laboratory, Argonne, Illinois 60439

C.-Y. Kim

Department of Materials Science and Engineering, Northwestern University, Evanston, Illinois 60208

G. Aeppli

NEC Research Institute, 4 Independence Way, Princeton, New Jersey 08540

N. D. Mathur and M. G. Blamire

Department of Materials Science, University of Cambridge, Cambridge CB2 3QZ, United Kingdom

E. D. Isaacs

Bell Laboratories, Lucent Technologies, Murray Hill, New Jersey 07974

Using x-ray submicrobeam, we spatially mapped the strain in epitaxial $\text{La}_{1-x}\text{Sr}_x\text{MnO}_3$ films grown on $\text{SrTiO}_3(001)$ bicrystal substrates. Our results show that there is an elastic strain gradient at the artificial grain boundary, which decays over a length scale of $\sim 1 \mu\text{m}$. The tensile strain at the interior of the grain—due to the lattice mismatch between $\text{La}_{1-x}\text{Sr}_x\text{MnO}_3$ and SrTiO_3 —relaxes as the film nears the grain boundary, yielding a grain boundary lattice constant which approaches the value of that in bulk $\text{La}_{1-x}\text{Sr}_x\text{MnO}_3$. © 2002 American Institute of Physics.

[DOI: 10.1063/1.1455609]

The observation of negative magnetoresistance in the ferromagnetic phase of polycrystalline manganites^{1–5} such as $\text{R}_{1-x}\text{A}_x\text{MnO}_3$ ($\text{R}=\text{La}, \text{Pr}, \text{Nd}$ and $\text{A}=\text{Ba}, \text{Sr}, \text{Ca}, \text{Pb}$) has drawn much attention recently due to the potential applications for magnetic field sensors. The phenomenon, which is characterized by an initial peak and rapid drop in the resistance at low fields followed by a slower decrease at higher fields, has been attributed to spin-polarized intergrain tunneling. Although spin-polarized tunneling can qualitatively explain the low field behavior in the resistance, details such as the gradual decrease of the resistance at higher fields have suggested the existence of a magnetically or electronically distinct region at the grain boundary.^{6,7} In this work, we present a local mapping of the strain at the grain boundary of an epitaxial $\text{La}_{0.7}\text{Sr}_{0.3}\text{MnO}_3$ film grown on a bicrystal $\text{SrTiO}_3(001)$ substrate using x-ray microdiffraction. Our previous measurements on this film using magnetic force microscopy^{8,9} have elucidated the existence of magnetically distinct regions at the grain boundaries with Curie temperatures higher than that in the bulk of the film,⁵ a phenomenon which we attributed to strain relaxation at grain boundaries. The current strain measurements by x-ray microdiffraction confirm that at the grain boundaries the strain relaxes, yielding a lattice constant different from the grain interior and accounting for the magnetic behavior observed by magnetic force microscopy.

Epitaxial $\text{La}_{1-x}\text{Sr}_x\text{MnO}_3$ films with $x=0.23, 0.3$ were grown by pulsed laser deposition on bicrystal $\text{SrTiO}_3(001)$ substrates with 45° misalignment. In this article, we use the pseudocubic notation to describe the crystal orientation of $\text{La}_{1-x}\text{Sr}_x\text{MnO}_3$. On one side of the grain boundary the $[100]$ axis is parallel to the grain boundary, whereas on the other side it is rotated by 45° with respect to the grain boundary around the surface normal. The growth procedure was similar to those reported previously where $\text{La}_{0.7}\text{Ca}_{0.3}\text{MnO}_3$ and $\text{La}_{0.7}\text{Sr}_{0.3}\text{MnO}_3$ films were grown on bicrystal $\text{SrTiO}_3(001)$ substrates for magnetotransport devices across artificial grain boundaries.³ Due to the lattice mismatch between $\text{La}_{1-x}\text{Sr}_x\text{MnO}_3$ ($a=b=c=3.88 \text{ \AA}$ for $x=0.3$) and the SrTiO_3 substrate ($a=b=c=3.905 \text{ \AA}$), these films are known to have a tensile strain,¹⁰ resulting in a suppression of the Curie temperature compared to the bulk,^{11,12} and a magnetization vector lying in the plane of the film.¹⁰ The degree of strain depends on the film thickness, where partial or complete relaxation of the strain can occur as the film thickness is increased.¹³

X-ray diffraction measurements to determine the crystal orientation, lattice constant, and thickness of the films were conducted at beam line X16B at the National Synchrotron Light Source at Brookhaven National Laboratory. The scattering data were collected with 7.60 keV energy photons. A beam size of $0.2 \text{ mm} \times 0.2 \text{ mm}$ was selected so that the incident x rays were confined to one domain of the film during the diffraction measurements. To determine the crystal orientation, we searched for the $(10L)$ and $(11L)$ diffraction

^{a)}Electronic mail: soh@research.nj.nec.com

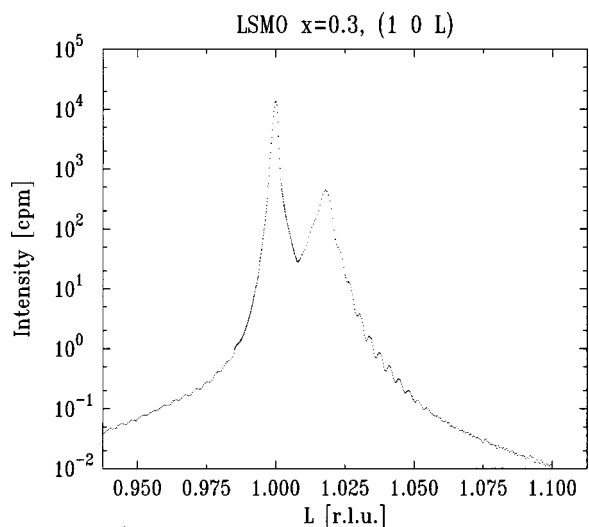


FIG. 1. X-ray diffraction (10L) scan of the $\text{La}_{0.7}\text{Sr}_{0.3}\text{MnO}_3$ film on SrTiO_3 showing the substrate peak at $L=1$ and the film peak centered at $L=1.018$, which gives a value of $c=3.836 \text{ \AA}$ for the surface normal lattice constant of the film. The periodicity of the interference fringes in the diffraction data corresponds to a film thickness of 1150 \AA .

peaks of the films. On one side of the grain boundary (domain A) the [100] axis is parallel to the grain boundary. On the other side (domain B) the [100] axis is rotated by 45° in the plane of the film. By comparing the crystal orientation information of the $x=0.23$ film with the magnetic domain images obtained previously on the same film,^{8,9} we infer that the magnetic domain walls occur along the $\langle 100 \rangle$ direction. The magnetic easy axes are deduced to be along the $\langle 100 \rangle$ direction¹⁴ from the ripple structure inside the magnetic domains, which are believed to have a texture orthogonal to the average magnetization direction.¹⁵

Figure 1 shows the (10L) rod profile for domain B for the $x=0.3$ film, which was obtained by varying the surface normal momentum transfer around the (101) substrate Bragg peak. The diffraction peak from the film is centered at $L=1.018$ ($L=1$ corresponding to the substrate peak). The average value of the surface normal lattice constant of the film obtained from various Bragg peaks is $c=3.842 \pm 0.002 \text{ \AA}$ (1.0% smaller than $c=3.88 \text{ \AA}$ of bulk $\text{La}_{0.7}\text{Sr}_{0.3}\text{MnO}_3$). The interference fringes in the diffraction data attest to the smoothness of the film and correspond to a film thickness of $1080 \pm 20 \text{ \AA}$. The intensities for in-plane momentum transfer measurements are centered at $H=1$ in the ($H 0 1.018$) scan and $K=0$ in the ($1 K 1.108$) scan, which means that the in-plane lattice constants of the film are the same as for the substrate.

We next proceeded to investigate the crystal structure at the grain boundary for the $x=0.3$ film using a submicron x-ray beam. The x-ray microdiffraction measurements were conducted at beam line 2-ID-D of the Advanced Photon Source at Argonne National Laboratory. A schematic drawing of the experimental setup is shown in Fig. 2, where a monochromatic 8 keV x-ray beam with a bandwidth of $\Delta\lambda/\lambda=2 \times 10^{-4}$ was focused to a submicron spot size at the sample. The focusing element for the x-ray beam is a Fresnel zone plate made by Au electroplating, which is supported on

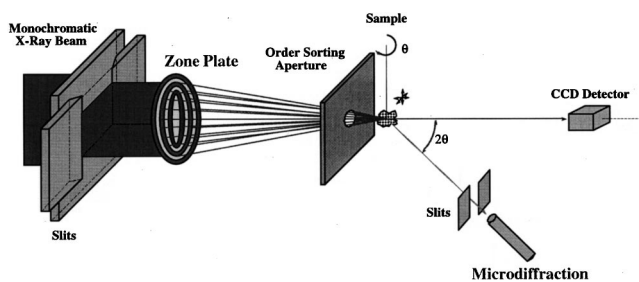


FIG. 2. Schematic drawing of the experimental setup for microdiffraction. A monochromatic x-ray beam is focused to a submicron beam size on the sample by a Fresnel zone plate. An order sorting aperture is inserted in front of the sample to select only the first order diffraction and reject higher order diffraction. The sample is mounted vertically with the grain boundary along the horizontal direction. The sample and the detector are rotated to meet the Bragg conditions.

a silicon nitride membrane.¹⁶ The zone plate has a diameter of $150 \mu\text{m}$, a thickness of $0.85 \mu\text{m}$, and a focal length of 100 mm at 8 keV , which means an upper bound of 0.086° for the divergence of the incident beam. The focused beam has an elliptical shape with the minor axis in the vertical direction. We measured an upper bound of $0.35 \mu\text{m}$ for the vertical width of the beam size at the sample location by detecting the K fluorescence of a Cr knife edge. The sample was mounted vertically on a sample stage with submicron translation control with the grain boundary running along the horizontal direction. This choice of the grain boundary orientation allows us a spatial resolution of $0.35 \mu\text{m}$ for microdiffraction in the direction perpendicular to the grain boundary (which we call y).

Using the focused submicron x-ray beam we looked at the (002) diffraction peak for the substrate and the film. Even though the film was grown on a $\text{SrTiO}_3(001)$ substrate, where nominally only the in-plane axes of the two domains were supposed to be misaligned, our measurements show that there is a slight difference ($\Delta\theta \sim 0.1^\circ$) in the orientation of the c axis between the two substrate domains and similarly between the two film domains on the opposite sides of the grain boundary. This slight difference in the tilt of the c axis is sufficient to enable us to locate the grain boundary by detecting the (002) substrate or film peak on either side of the grain boundary and seeing it disappear as the beam crosses to the other side of the grain boundary as the sample is scanned vertically along y . The location of the grain boundary is determined by the condition that the intensity of the (002) reflection drops halfway from its maximum value. The grain boundary location determined this way by the two substrate peaks and two film peaks are within $2 \mu\text{m}$ of each other, the difference arising from the hysteresis of the translational motion of the stage.

In order to study the lattice constant of the film around the grain boundary, we did two-dimensional ($\theta-2\theta, y$) scans for the substrate and film peaks for both domains. The results for domain A are displayed in Fig. 3, with the $\theta-2\theta$ axis converted into a surface normal lattice constant. Similar results were obtained for domain B as well. The 2θ value at the substrate peaks were used to calibrate the 2θ angle of the goniometer from the known value of $c=3.905 \text{ \AA}$. The width

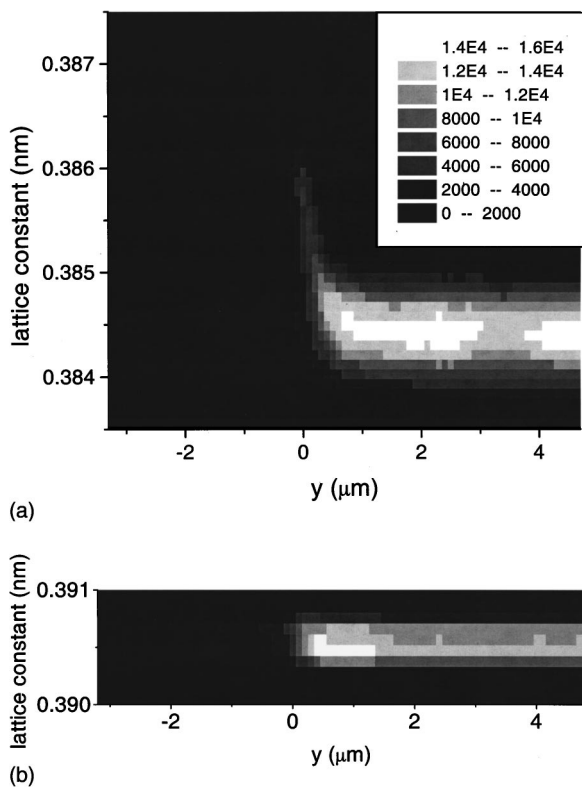


FIG. 3. Two-dimensional ($\theta-2\theta, y$) scans of (a) the $\text{La}_{0.7}\text{Sr}_{0.3}\text{MnO}_3$ film and (b) the SrTiO_3 substrate in one of the domains. $y=0$ is the position of the grain boundary.

of the substrate peak is determined by the resolution in 2θ , which was $\sim 0.06^\circ$ (equivalent to 0.005 \AA resolution in lattice constant) in our setup. The two-dimensional substrate peak scans [Fig. 3(b)] show that the substrate lattice constant is not spatially dependent. On the contrary, the same experiment on both film peaks (domain A and B) show a drastically different effect: the c lattice constant increases as we approach the grain boundary.

The tensile strain, which results in a reduced surface normal lattice constant of 3.845 \AA at the grain interior from the bulk value of 3.88 \AA , relaxes near the grain boundary. This results in an enhanced surface normal lattice constant of

3.865 \AA (domain B) and 3.86 \AA [domain A, Fig. 3(a)] compared to the grain interior for the two domains opposite to the grain boundary. The current results are in line with our previous magnetic force microscopy measurements which showed the existence of distinct mesoscopic regions at the grain boundaries with Curie temperatures higher than the grain interiors,^{8,9} a phenomenon which we attributed to strain relaxation at grain boundaries. The length scale over which the strain relaxes is $\sim 1 \mu\text{m}$, similar to the length scale of the mesoscopic magnetism.

In summary, we have presented x-ray microdiffraction as a powerful tool to study lattice distortion effects at grain boundaries in manganite films. In particular, using this local probe we discovered local variation of strain by as much as 0.5% at the grain boundaries in epitaxially grown $\text{La}_{0.7}\text{Sr}_{0.3}\text{MnO}_3$ films.

The authors acknowledge valuable discussions with V. K. Vlasko-Vlasov, Ch. Renner, and Frank M. Zimmermann.

¹H. L. Ju, J. Gopalakrishnan, J. L. Peng, Q. Li, G. C. Xiong, T. Venkatesan, and R. L. Greene, *Phys. Rev. B* **51**, 6143 (1995).

²H. Y. Hwang, S.-W. Cheong, N. P. Ong, and B. Batlogg, *Phys. Rev. Lett.* **77**, 2041 (1996).

³N. D. Mathur *et al.*, *Nature (London)* **387**, 266 (1997).

⁴K. Steenbeck, T. Eick, K. Kirsch, K. O'Donnell, and E. Steinbeiß, *Appl. Phys. Lett.* **71**, 968 (1997).

⁵R. Mathieu, P. Svedlindh, R. A. Chakalov, and Z. G. Ivanov, *Phys. Rev. B* **62**, 3333 (2000).

⁶J. E. Evetts, M. G. Blamire, N. D. Mathur, S. P. Isaac, B.-S. Teo, L. F. Cohen, and J. L. MacManus-Driscoll, *Philos. Trans. R. Soc. London, Ser. A* **356**, 1593 (1998).

⁷D. J. Miller, Y. K. Lin, V. Vlasko-Vlasov, and U. Welp, *J. Appl. Phys.* **87**, 6758 (2000).

⁸Y.-A. Soh, G. Aeppli, N. D. Mathur, and M. G. Blamire, *J. Appl. Phys.* **87**, 6743 (2000).

⁹Y.-A. Soh, G. Aeppli, N. D. Mathur, and M. G. Blamire, *Phys. Rev. B* **63**, 020402 (2001).

¹⁰C. Kwon *et al.*, *J. Magn. Magn. Mater.* **172**, 229 (1997).

¹¹A. J. Millis, T. Darling, and A. Migliori, *J. Appl. Phys.* **83**, 1588 (1998).

¹²Q. Gan, R. A. Rao, C. B. Eom, J. L. Garret, and M. Lee, *Appl. Phys. Lett.* **72**, 978 (1998).

¹³R. A. Rao, D. Lavric, T. K. Nath, C. B. Eom, L. Wu, and F. Tsui, *Appl. Phys. Lett.* **73**, 3294 (1998).

¹⁴Y. Suzuki, H. Y. Hwang, S.-W. Cheong, and R. B. van Dover, *Appl. Phys. Lett.* **71**, 140 (1997).

¹⁵A. Hubert and R. Schäfer, *Magnetic Domains* (Springer, Berlin, 1998).

¹⁶B. Lai *et al.*, *Appl. Phys. Lett.* **61**, 1877 (1992).